Rachid Zegait[1], Zekai Şen[2], Antonio Pulido-Bosch[3],
Housseyn Madi[4], Bachir Hamadeha[5]

Flash Flood Risk and Climate Analysis in the Extreme South of Algeria (the Case of In-Guezzam City)

Abstract: Natural risks, particularly flood risk, are a topical subject in Algeria and throughout the world, particularly given the last major catastrophic floods in Sudan (2020) and North Africa. With the development of the climate change phenomenon in the world, risk management is becoming increasingly necessary for all the actors concerned (decision-makers, technicians, and the population) to identify protection issues. In 2018, in the extreme south of Algeria, In-Guezzam City suffered a devastating flood that caused significant damage and loss of human and material resources. More than 100 homes collapsed, and approximately 345 families were displaced. Currently, there is no research work to assess the hydrological situation and the risk of flooding in this region. Therefore, the main purpose of this study is to shed light on the risk of flash floods in the extreme south of Algeria with more specific attention to the August 2018 floods as well as the climate trends over the past 30 years using Mann–Kendall test and Sen's Slope Estimator. The chosen approach involves a hydrological study and hydrodynamic modeling using HEC-RAS software. This latter allows for simulating floods using statistical methods and creating several regional flood hazard maps.

Keywords: climate trend, flash floods, HEC-RAS, modeling, risk analysis

[1] University of Djelfa, Faculty of Science and Technology, Hydraulic Department, Djelfa, Algeria, email: zegait.rachid@gmail.com, https://orcid.org/0000-0001-7976-0595
[2] Istanbul Medipol University, Engineering and Natural Sciences Faculty, Istanbul, Turkey, King Abdulaziz University, Center of Excellence for Climate Change Research / Department of Meteorology, Jeddah, Saudi Arabia, email: zsen@medipol.edu.tr, https://orcid.org/0000-0001-9846-8581
[3] University of Granada, Department of Geodynamics, Granada, Spain, email: apulido@ual.es, https://orcid.org/0000-0001-7409-1572
[4] University of Tamanrasset, Department of Science and Technology, Tamanrasset, Algeria, email: housseyn_madi@yahoo.fr, https://orcid.org/0000-0003-2041-8722
[5] University of Tamanrasset, Department of Science and Technology, Tamanrasset, Algeria, email: ham_bachir@ymail.com

1. Introduction

The causes behind climate change are difficult to identify. They can manifest themselves through long periods of drought or flash floods with adverse effects on the hydrological cycle and environmental and socioeconomic activities [1–3].

Different types of flooding, namely fluvial flood (FF) and pluvial flash flood (PFF), typically occur in urban regions located next to rivers [4, 5]. The notion of flash floods is not recent; they are defined as violent and short-lived floods generated by intense storms that are particularly damaging. They generally lead to natural hazards worldwide due to their multidisciplinary nature of difficulty in forecasting and rapid reaction [6–8]. For this reason, they are considered the most destructive natural phenomenon and pose the greatest threat to human life [9, 10]. This type of phenomenon is often very localized and affects small watercourses. Over the last ten years, it has been the subject of renewed interest worldwide. The latest European research calls for tenders in the environmental field included articles specifically dedicated to the study, prevention, and forecasting of flash floods, except for any other type of flood. With the same interest, the European Regional Flood Management Program of the World Meteorological Organization focused on flash floods [11]. Historically in Europe, among the most critical floods recorded in Europe: in Lynmouth in Great Britain in 1952 (34 victims), Barcelona in 1962 (more than 400 victims), the Piedmont region in Italy in 1968 (58 victims), and the Aude flood in 1999 with 35 victims [11]. In recent years, the Reinosa floods (Cantabria, Spain) in January and December 2019, the second in December, were among the worst floods in history. The researchers are talking about a discharge of 246 m^3/s in 15 minutes [12]. On November 15, 2017, a high-intensity convective storm, reaching 300 mm in the core zone of the event, hit the western part of Attica in Greece. This storm caused a catastrophic flash flood in the town of Mandra and a tragic loss of 24 people, making it the most deadly flood in the country in 40 years [13]. In North Africa and the Arabic region, in Chad 2012, floods displaced hundreds of thousands of people and submerged 255,720 ha of cultivated land, where several hundred families from the capital N'Djamena were displaced to higher lands [14]. In Egypt, flash floods in January 2010 in Wadi El Arish and January 2013 in Qena caused massive damage to materials and humans [15].

In September 2020, violent floods affected almost all of Sudan (106 victims), thousands of hectares were also destroyed, and more than 500,000 inhabitants were affected [16]. Financial losses and material damages are generally very high; 300 million euros for the city of Nîmes alone in 1988 (Ville de Nîmes, 1989), 1.2 billion euros in the Gard region in 2002 [17], and 3.3 billion euros in Aude 1999 [18]. These values should be compared with the average annual number of insured losses related to natural disasters worldwide, that is, around 40 billion euros [19].

Like many other countries, Algeria has experienced several devastating floods, primarily known for overflowing large rivers in the extensive agricultural plains. During the last 20 years, they have mainly affected the major cities and urban centers

(Algiers 2001, Bejaia 2012, and Batna 2020), where they have caused many losses of life and considerable material damage. In this regard, climate variability is considered one of the main causes of these devastating floods, as different models have predicted a likely increase in precipitation and temperatures in several regions of the world [20, 21]. Therefore, the emergence of many recent climatic phenomena has prompted the world community to take an interest in climate change and its impacts on water resources. These include droughts that have affected Maghreb countries and Algeria, especially since the 1970s, and were sometimes followed by devastating floods [22, 23].

Several studies have been conducted in the northern regions of Algeria about rainfall and temperature [24]. According to Bessaklia [25], in the extreme northeast of Algeria, through 23 rainfall stations, the Mann–Kendall test showed areas with increasing trends in high precipitation events. On the other hand, there appear to be more droughts occurring in the arid and semi-arid areas in northeastern Algeria. At the same time, humid and sub-humid locations received more precipitation and consequent floods [26]. In southern Algeria, few works analyzed the climate change effects on water resources, except for some works by Remini in 2020, where he showed that it is necessary to adapt hydraulic systems to a dry climate based on traditional systems used for centuries. Historically in the Algerian Sahara, where aridity is the central element [27], floods are highly beneficial because they are the main source of groundwater recharge along drainage basins [28]. However, in recent years, severe floods have occurred in these areas, causing economic losses and deaths. They often result from torrential rains such as Tamanrasset in 2002, Adrar in 2004, Illizi in 2006, Ghardaïa in 2008, In-Guezzam in 2018, and Djanet in 2019 [29, 30]. These devastating floods are due to complex weather phenomena such as climate change. They represent the most widespread Mediterranean disasters [31].

According to records, In-Guezzam City was exposed to four significant floods and more violent events in 1997, 2000, 2015, and 2018 [30]. Historical flood disasters worldwide and the evolution of built-up habitats in flood-prone areas are key drivers for avoiding flood risks. Our contribution is part of this context, and our reflections focus on the problem of floods in Algeria.

The **main aim** of this study is to shed light on the flash flood risk in the extreme south of Algeria through a hydrological and hydraulic modeling study with particular attention to the floods in August 2018 and the 30-year climate trend. Since there is no research study to evaluate the hydrological situation in this region, the main **novelty** is that this study is recognized as the first study that will contribute greatly to a better understanding of the flooding process on the Algerian-Nigerian border. This research can be used as fundamental information for researchers, emergency planners, and managers to identify protection problems in these regions.

2. Study Area

The study area is located in the extreme south of the Algerian Sahara, on the continuation of the National Road N°1 that connects Algiers to Tamanrasset (Fig. 1a)

and then to the border with Niger at the coordinates 19°34′07″ north, 5°46′20″ east. In-Guezzam City (Fig. 1b) is located more than 2,000 km from the capital and 400 km from the central province of Tamanrasset. It is considered a transition point between Algeria and African countries, administratively covering more than 46,000 km², or 8.40% of the total area of Tamanrasset province. The climate is hyperarid according to the different climatic parameters (temperature, rainfall, wind, evaporation, humidity) (1988–2018) provided by the National Meteorological Office in 2019. It is characterized by low rainfall and irregular with an average of around 30 mm/year and high temperatures during the summer, which can exceed 45°C. In winter, it is generally mild with average temperatures (10–20°C). Winds are relatively frequent and irregular and play an essential role in the formation of ergs and regs [32]. Their speed is important from April to July, which causes the sirocco and sand winds during this period, accompanied by a robust evaporation rate (around 6,621 mm/year) [33].

The In-Guezzam watershed is an integral part of Tassili Hoggar, whose main features are the extent of its rocky plateaus sporadically strewn with dunes. It is located in the depression area of Sahb El-Rahala and Adakh-Adakh watercourses, which represent the main drain of the basin with a length of 20 km and 24 km, respectively. It covers an area of 170 km² (Tab. 1). The flat geometry of the In-Guezzam area and the absence of banks (significant bed limits) with the extended width of the main watercourses led to the disappearance of traces after the floods [34]. It is gradually fed throughout its course by small sources (Fig. 1d, e). Its low flow rate is zero, despite its large catchment area. The watershed has a low drainage density. The value calculated according to Horton's law (1945) is 1.65, the average slope of the watershed is 0.35%, and it evokes a medium roar. The vegetation cover is almost non-existent except for some trees at the bottom of the watercourse. Runoff promotes soil stripping and the dismantling of terraces at the bottom of valleys. The high density of In-Guezzam urbanization often settles in the lowest catchment areas, which led to the exposure of urban expansion to the risk of flooding and has made a thorny development problem, requiring adequate planning tools and effective interventions.

Table 1. Physiographic parameters of the In-Guezzam watershed

Watershed	A [km²]	P [km]	K_G	Max altitude	Min altitude	Average slope [%]	L_{cp} [km]
SahbEl-Rahala	71.02	67.34	2.24	497	387	0.35	19.98
Adakh-Adakh	98.20	85.99	2.45	529	387	0.35	24.14

Explanations: A – sub-watershed area, P – sub-watershed perimeter, K_G – Gravelius index, L_{cp} – main-stream length.
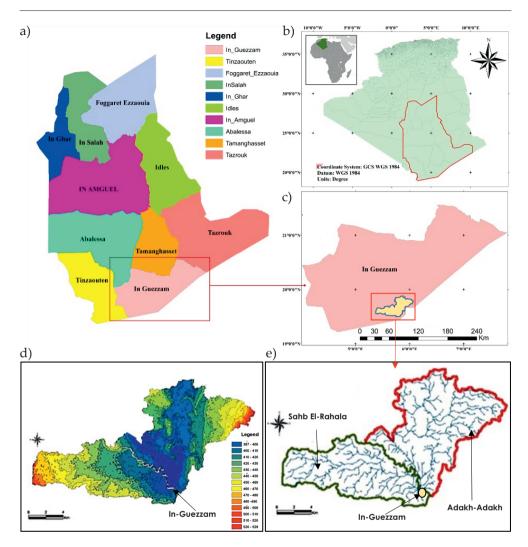
Fig. 1. In-Guezzam region (a); state of the Tamanrasset region (b); situation of the study area (c); hypsometric map of Sahb El-Rahala and Adakh-Adakh watercourses (d); hydrographic network map (e)

3. 2018 In-Guezzam Floods

In the extreme south of Algeria, In-Guezzam City was exposed in 2018 to an extreme flood, accompanied by violent storms, which began on Saturday, 4 August 2018, after many years of drought. It rained almost 53 mm in a few hours [33], generating an increase in water level in the main watercourses of the region at full speed [33] and causing significant damage to human and material resources (Fig. 2).

According to the In-Guezzam civil protection declarations, this flood severity was considered the first since 1997; all city areas were flooded on the first day with over 272 ha (i.e., 41% of the total urban area); more than 100 houses collapsed, and about 345 families were displaced.
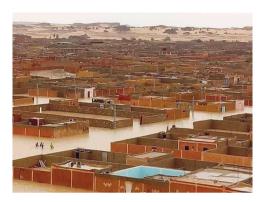

Fig. 2. Examples of damage caused by the August flood of 2018
(photo by R. Zegait, 2018)

4.   Data Used

4.1.   Meteorological Data

The required climatic data (Tab. 2) of the study area referring to precipitation and temperature were obtained from the regional meteorological station of In-Guezzam (05°46′E, 19°34′N), established and managed by the National Meteorological Office (ONM). The 30-year time series (1988–2018) was complete without missing values; it was and provided daily measurements for precipitation and temperature [mean, maximum (max), and minimum (min) values]. All data sets have been geo-referenced according to the UTM projection (zone 31), WGS84 Datum.

Table 2. Statistical characteristics of the data

Parameter	Min	Max	Mean	Deviation	CV
P_{total}	0.40	138.00	31.30	31.90	1.02
T [°C]	28.03	30.84	29.19	0.63	0.02
$P_{d\,max}$	0.40	60.00	17.90	17.14	0.96

4.2. Satellite Images and Weather Conditions of the 2018 Floods

The extreme south of Algeria, northern Mali, and Niger were battered by a thunderstorm from August 2 to 4, 2018. The storm caused severe weather that led to catastrophic floods. Past weather conditions can be summarized based on Meteo-sat infrared images and weather reports as follows (Fig. 3)
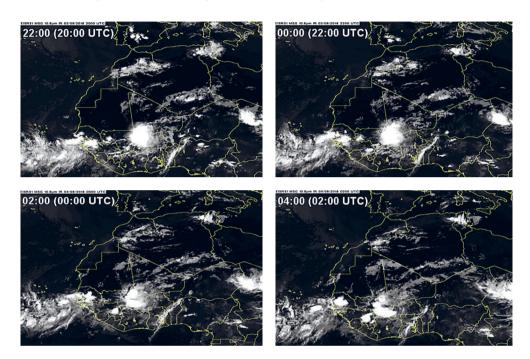

Fig. 3. Infrared images show the 6 hours of development of jet streams over the Sahara from August 3, 2018 (22:00 UTC) to August 4, 2018 (04:00 a.m. UTC)

The storm originated in the Atlantic Ocean, the Gulf of Senegal, and Guinea-Bissau. It passed through the countries of West Africa as it spread in the middle of Mali, then headed towards the far south of Algeria, specifically the In-Guezzam region, where the Algerian-Nigerian border area was affected by heavy rains (>53 mm), then the intensity of the clouds decreased. From the evening of August 4, 2018 the storm moved to northern Niger and Chad.

In the same context, the Algerian Space Agency has programmed images of the Alsat-1B and Alsat-2 Earth observation satellites. This action was done to assess and highlight the Spatio-temporal evolution of the flood. Three satellite images are taken on different dates. Figure 4 represents one of the satellite images extracted from the Alsat-1B high-resolution sensor on August 7, 2018. It shows the spatial extent of the flood in 72 hours (480 ha) in the lowlands that distinguishes the In-Guezzam region.
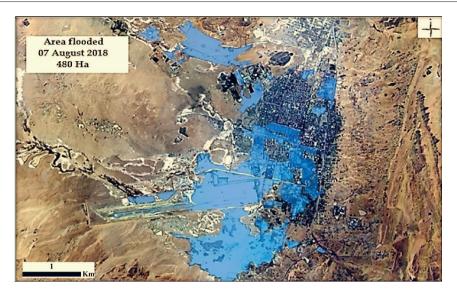
Fig. 4. Global view of the flooded city of In-Guezzam from Alsat-2 satellite imagery of
August 7, 2018 (false color mode)

5.   Methodology

5.1.   Climate Trend

A trend analysis of mean annual temperature values and precipitation data was applied to perform the Mann–Kendall test [35, 36] and Sen's slope [37] to investigate whether there has been a significant trend (increase or decrease) in climatic conditions during the last 30-year period. This technique recognizes any trend in a given time series without specifying whether the trend is linear or not [38].

Mann–Kendall test

The Mann-Kendall (MK) statistical test has been widely applied in the trend detection of the hydrometeorological time series. This test is characterized by accepting missing values from time series [39, 40]. The MK trend test is based on two hypotheses; one is null (H_0), and the other is an alternate hypothesis (H_1). While H_0 states no trend, H_1 explains a significant increase or decrease in precipitation data [41].

The S-test statistic is defined by Taxak et al. [42] as follows:

$$S = \sum_{i=2}^{n}\sum_{j=1}^{i-1}\mathrm{sgn}(x_i - x_j) \tag{1}$$

where:

x_i, x_j – sequential data values,
n – length of data set;

$$\text{sgn}(x_i - x_j) = \begin{cases} 1, & \text{for } (x_i - x_j) > 0 \\ 0, & \text{for } (x_i - x_j) = 0 \\ -1, & \text{for } (x_i - x_j) < 0 \end{cases} \tag{2}$$

When $n \geq 8$, it is documented that the S statistic is approximately normally distributed with mean $E(s) = 0$ and its variance as:

$$\text{Var}(S) = \frac{1}{18}\left[n(n-1)(2n+5) - \sum_{p=1}^{q} t_p(t_p - 1)(2t_p + 5) \right] \tag{3}$$

where:

q – number of tied values,
t_p – number of ties for p^{th}-value.

A Monte Carlo simulation was used to evaluate the statistical significance of the trends at the 5% of the significance level. At this level, a positive (negative) trend is significant when the p-value >0.05 (<0.05) [43]. The null hypothesis H_0 assumes no trend in the series, meaning that the data series is homogeneous [44].

Sen's slope estimator

Sen's slope developed by Sen [37] has been widely used to calculate the magnitude of trends in the long-term temporal data [45–48]. In this study, Sen's slope is applied to calculate the magnitude of the trend for temporal data. Sen's slope is considered better for detecting linear relationships as it is not affected by outliers in the data.

Slope values of positive Sen show an increasing trend, while slope values of negative Sen tell us that there is a negative trend in temporal data. Sen's slope is given by the following expression [49]:

$$\beta = \text{mediane}\left[\frac{(x_j - x_k)}{(j-k)} \right], \text{ for } k < j \tag{4}$$

where $1 < k < j < n$, and β is the data set's median of all possible pair combinations.

5.2. Hydrological Study

The flood magnitude modeling and measurement scheme are based on two studies, namely hydrological studies, which aim to estimate peak flows corresponding to the different return periods at the project area level. Peak flow calculations are required for flood control studies in water engineering [50]. The relationship between precipitation and peak flow plays a fundamental role in all hydrological applications [51, 52], such as engineering design [53], flood forecasting [54, 55], and evaluation effects of best management practices in the watershed [56].

The following steps are considered for the completion of the study:

1. Finding past flood leads and collecting testimonials from dwellings at the most appropriate locations. As a result, In-Guezzam City was exposed to the most critical floods in 1997, 2004 and 2018.

2. Statistical analysis was performed via several statistical distribution tests (Exponential (L-Moments), Log Pearson III, EV3-Min (Weibull), GEV-Min (L-Moments), EV3-Min (Weibull, L-Moments)) using the Hydrognomon software [57]. All selected tests were subjected to χ^2, and Kolmogorov–Smirnov tests to determine the optimal probability distribution function (PDF) of maximum daily precipitation and the P_d peak for a T return period ranging from 5 up to 1,000 years. This method is generally preferred by researchers and designers, especially for appropriate numbers of data [58], because it is easy to apply and is often statistically efficient; it applies to basins receiving homogeneous precipitation, with a few tens to several thousand square kilometers.

3. For each return period, the precipitation amounts corresponding to a short time (less than 24 h) are determined by the formula (5) developed at the request of the National Hydraulic Resources Agency (NHRA) by [59]:

$$P_t = P_{d_{max}} \left(\frac{t}{24} \right)^b \tag{5}$$

where:

t – concentration time [h],

b – climatic exponent,

$P_{d_{max}}$ – daily maximum precipitation frequency.

4. Estimation of concentration time using the most common empirical formulas in Algeria (Giandotti, Californian, Kripich, and Ventura). This study is based on the Californian formula (6) as it fits firmly with the data collected through in-site surveys:

$$T_c = \left(\frac{0.87 \cdot L^3}{H_{max} - H_{min}} \right)^{0.386} \tag{6}$$

where:

L – main watercourse length [km],

H_{max}, H_{min} – respectively, maximum and minimum height of the watershed [m].

5. Estimation of flood flows with different empirical formulas (Mallet-Gauthier, Turazza, Giandotti, and Sokolovsky). They adapted to the nature of the watershed as written in the Giandotti formula (7) and took into account the size and topographical slope of the watershed,

$$Q_{max,p\%} = \frac{C \cdot A \cdot h_{tc,p\%} \sqrt{h_{mean} - h_{min}}}{4\sqrt{A} + 1.5L} \tag{7}$$

where:

L – main watercourse length [km],

h_{mean}, h_{min} – respectively, mean and minimum height of the watershed [m],

A – watershed area [km²],

$h_{tc,p\%}$ – a layer of precipitation water layer for a given probability and a duration that is equal to the concentration-time,

C – topographic coefficient ranging from 66 to 166.

6. Flood hydrograph estimation.

5.3. Modeling

The second part requires hydraulic modeling followed by a simulation phase of the In-Guezzam watercourse. First, the essential elements for the hydraulic modeling process were provided, then the identification of flood risk areas. The last one is done by following five steps:

1. Identification of the geometry of the watercourse, where hydraulic modeling requires a finer spatial scale. Thus, the calculation accuracy of water-surface elevation is closely on the accuracy of the topographic data. Due to the absence of high spatial resolution topographic maps for In-Guezzam City, this study has been based on a topographic survey (Fig. 5) carried out by a consulting company as part of a hydraulic study in In-Guezzam [60] using a Leica-TS06 which can perform measurements with high accuracy.

2. Identification of data for each session using Manning coefficient according to the soil nature.

3. Identification of flow rates and boundary conditions.

4. Identification of the calculation conditions (height of the water, critical depth, hydrograph, limn-graph, depending on the flow regime).

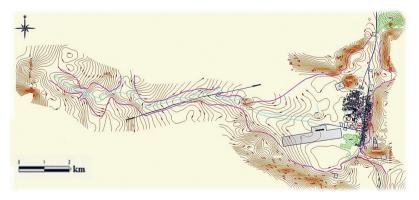5. Visualization of the results in graphic forms and tables.

Fig. 5. Topographic survey of the In-Guezzam region
Source: [60]

During this study, two software packages were used: a Geographic Information System (ArcGIS) and a River Modeling Software (HEC-RAS), which was developed at the Hydrologic Engineering Center of the US Army Corps of Engineers [61]. This software has already proven to be very efficient for this type of study; many companies and research laboratories consider it a first-rate tool.
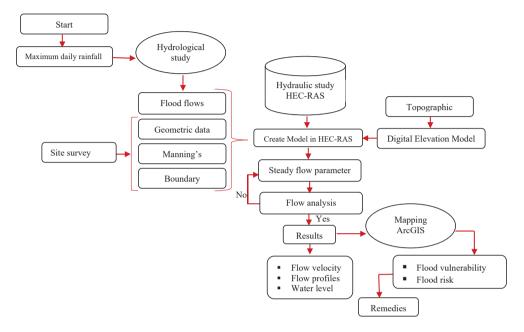

Fig. 6. Methodology flow chart

The calculations of gradually varying water flow lines are based on Bernoulli's equation. The load losses are evaluated by the Manning-Strickler equation for the friction term and the contraction-expansion coefficients. In an abruptly varied flow, HEC-RAS uses the momentum equation (Fig. 6).

6.   Results and Discussions

6.1.   Climate Trend Analysis

In the past, Algeria has experienced several droughts. This fact draws our attention to the magnitude of the rainfall deficit recorded throughout the territory, particularly in the country's west.

The following analysis is based on synthesizing recent climate changes and projections in In-Guezzam. According to Figure 7a, the annual temperatures range from 28.0°C (1992) to 30.8°C (2010). The coldest years are 1989, 1992, and 1994,

respectively. The warmest years are 1998, 2005, and 2010. On the other hand, annual rainfall (Fig. 7b) ranges from 0.4 mm (2001) to 138 mm (2018). In 1992, 2001, and 2006, minimum rainfall heights were recorded. In contrast, years with maximum rainfall heights are 1997, 2000, 2010, 2015, and 2018.

a)

b)

Fig. 7. Graphical representation of the sequential trend using Sen's slope for mean annual temperatures (a) and annual precipitation (b)

The results of the Mann–Kendall test (Tab. 3) show that the alternative hypothesis H_1 is accepted for all series tested (p-value < 0.05), annual mean temperature (0.0001); and total annual precipitation (0.0368); series present a certain homogeneity of the data at the 5% significance level. The climatic parameters of the studied station have statistically **significant trends**.

Table 3. Results from Mann–Kendall's trend test

	MK statistics	Kendall's tau	Var(S)	p-value (two-tailed)	Model interpretation
Mean annual T [°C]	245	0.5632	0.00	<0.0001	accept H$_1$
Annual rainfall [mm]	118	0.2716	3,140.67	0.0368	accept H$_1$

According to Sen's slope estimates at the 5% significance level (Tab. 4), all parameters examined showed significant positive trends over the last 30 years, where the magnitude of warming is very significant, presented with a positive trend on the annual average (Sen's slope = +0.0512°C/year). This significant warming is mainly due to the steadily increasing summer average worldwide.

The general rainfall trend in Algeria is decreasing except for some Saharan regions such as In-Guezzam, where a positive trend lasts 30 years (Sen's slope = +1.175 mm/year).

Table 4. Sen's slope value

	Sen's slope	Confidence interval
Mean annual temperatures	0.0512	(−0.2251; 0.2529)
Annual rainfall	1.175	(−10.7083; 17.5450)

6.2. Hydrological Study

Statistical analysis is performed on time series using Hydrognomon software to calculate the 24-h maximum precipitation. Statistical distributions are subjected to the χ^2 test and the Kolmogorov–Smirnov test to assess how well they fit the time series, taking into account the concern about the effect of the time series length on distribution performance. The distributions that best fit the time series are EV3-Min (Weibull, L-Moments) (Extreme Value-min; Fig. 8, Tabs. 5, 6).

Table 5. Distributions performance subject to test

Statistical distributions	χ^2 test				
	a = 1%	a = 5%	a = 10%	attained a [%]	Pearson parameter
Exponential (L-Moments)	accept	accept	accept	60.65	1
Log Pearson III	accept	accept	accept	31.73	1
EV3-Min (Weibull)	accept	accept	accept	51.34	1.33333
GEV-Min (L-Moments)	accept	accept	accept	41.42	0.66667
EV3-Min (Weibull, L-Moments)	accept	accept	accept	84.65	0.33333

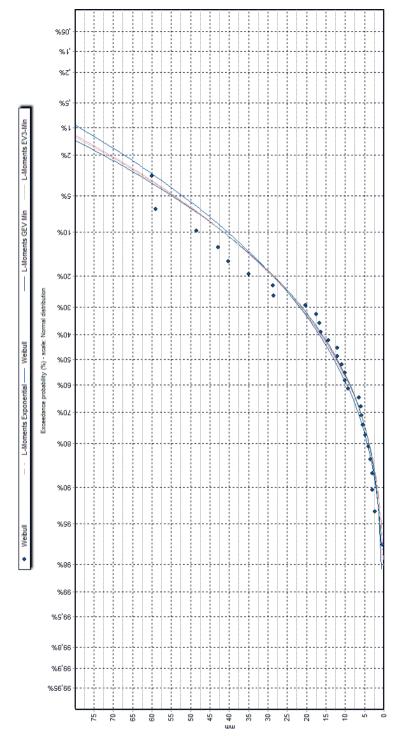**Fig. 8.** 24-h maximum annual precipitation shown in a normal distribution plot with tested distributions

Table 6. Distribution performance subject to Kolmogorov–Smirnov test

Statistical distributions	Kolmogorov–Smirnov test				
	$a = 1\%$	$a = 5\%$	$a = 10\%$	attained a [%]	D_{max}
Exponential (L-Moments)	accept	accept	accept	99.52	0.06861
Log Pearson III	accept	accept	accept	89.47	0.09782
EV3-Min (Weibull)	accept	accept	accept	99.50	0.06881
GEV-Min (L-Moments)	accept	accept	accept	99.95	0.05827
EV3-Min (Weibull, L-Moments)	accept	accept	accept	99.76	0.06488

According to the analysis, the maximum 24-h precipitation for the return periods of 10-year, 20-year, 50-year, and 100-year are 41.60 mm, 54.46 mm, 71.56, and 84.56 mm, respectively.

The hydrological study aims to evaluate flood flows for return periods of 5, 10, 20, 50, 100, and 1,000 years. The return period corresponding to one year ($T = 1$ year) was not considered, as the corresponding rainfall is below the runoff threshold, estimated at 5 mm [34].

The precipitation analysis focuses on the development of intensity-duration-frequency (IDF) curves. The IDF curves are plotted for the different return periods of 5, 10, 20, 50, 100, and 1,000 years (Fig. 9). The rainfall intensity is selected from the IDF curve. These curves are generated from the point precipitation data collected in the local area by fitting the maximum daily precipitation intensities for a specified duration to EV3-Min (Weibull, L-Moments), usually by plotting the data on a normal value probability paper [62].
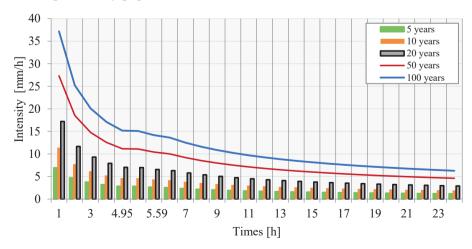

Fig. 9. Intensity-duration-frequency (IDF) curves

6.3. Concentration Time / Flow Rates

The concentration time of two sub-watersheds (Sahb El-Rahala, Adakh-Adakh) was estimated by 4.95 h and 5.59 h respectively. It can be noted that this concentration time is relatively high, which can be explained by the elongated shape of the sub-watersheds and the low slopes that reign there.

The regional knowledge of surface runoff is essential to the study of floods. However, the poor quality of the observed data (unavailable, discontinuous, accompanied by measurement or data entry errors) makes it difficult to quantify the flow rates.

In this regard, using empirical formulas that can transform rainfall into runoff through the morphological characteristics of the watersheds is among the most widely used methods in Algeria [63].

The flows selected from the analysis and the comparison of the calculated flows by the various methods (Mallet Gauthier, Turazza, Giandotti, and Sokolovsky) are summarized in Table 7.

Table 7. Flows rates estimated by different regional methods

Return period [year]	Mallet-Gauthier [m^3/s]	Turazza [m^3/s]	Giandotti [m^3/s]	Sokolovsky [m^3/s]
1,000	148.73	1381.82	391.07	1,295.27
100	118.86	548.64	162.76	514.41
50	108.26	378.15	119.43	354.45
20	92.41	222.34	79.34	218.02
10	78.32	136.88	49.99	128.34
5	61.05	76.87	30.44	72.05

The results of the Giandotti formula (4) can be chosen because this formula considers all the characteristic parameters of the watershed. In addition, the results are very close to the recorded flow floods of the watercourses around the region [64].

6.4. Flood Hydrographs

To define a typical flood hydrograph of a watercourse, the most representative floods inventoried by their peak times and peak flows are "scaled up" and superimposed on typical hydrographs. The USSCS hydrograph is adopted; it is a dimensionless unit hydrograph (Fig. 10), with base time and peak flow as input. The mounted time is 4.95 h for the **Sahb El-Rahala** watercourse and 5.59 h for the **Adakh-Adakh** watercourse, while the base time is 2.5 times the rising time (Fig. 10).
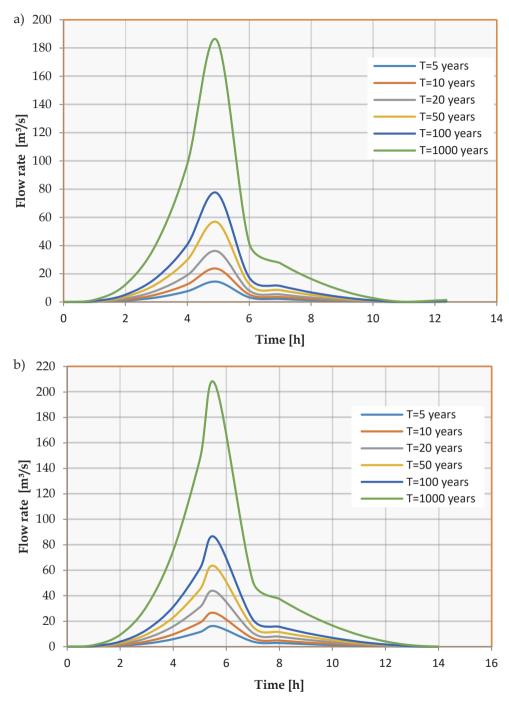
Fig. 10. Flood hydrograph for different return periods:
a) Sahb El-Rahala watercourse; b) Adakh-Adakh watercourse

6.5. Hydraulic study

The permanent regime remains the simplest and the most satisfactory for the hydraulic model realization of **Sahb El-Rahala** and **Adakh-Adakh** watercourses. A hydraulic model was designed to identify the flood's impact and behavior downstream of the watercourses at the western and northern of In-Guezzam City. The topographical data form is considered the basis for all fluvial hydraulic modeling. In this regard, 22 topographic profiles have been identified on 15 km of the watercourse. The chosen profiles are perpendicular to the direction of the flow; they do not cross between them, intersect the whole alluvial plain and take into account the geomorphological modifications of the major bed.

The bed roughness coefficient makes it possible to have the closest model to reality by considering the water speed at the bottom of the watercourse and the banks. On each cross-section profile, the Manning coefficient will be set to 0.033 for both banks. This value corresponds to the standard value for a river composed of coarse particles (pebbles) [65].

The peak flows, Q_p, selected from the hydrological study appear as the results of an analysis and a comparison of the flows calculated for different return periods (Tab. 8).

Table 8. Flow of return periods necessary for modeling

T [year]	5	10	20	50	100
Q_p [m³/s]	30.44	49.99	79.34	119.43	162.76

Hydrological data have boundary conditions. For the steady-state simulation, the flow is constant, and the HEC-RAS simulation considers only one flow in the river. The swallowing condition imposed on the model is a known water level rating of 2 m.

The system was modeled after the 2018 flood, the last significant flood of the **Sahb El-Rahala** watercourse. The calibration of a model is done after several simulations by varying Manning's coefficient.

6.6. Hydrodynamic Modeling

Hydraulic modeling consists of simulating the flow of a stream. The result of this simulation provides the spatially identifiable potential flood zones (hazard map), i.e., the riskiest areas to the population (risk map) during heavy floods of the surrounding rivers. These maps are based on hydrological studies, ArcGIS, and HEC-RAS software. The drawn-up maps show the different flood zones for each return period. One can note that the fifties, centennial, and millennial floods submerge a surface, as indicated in (Figs. 11, 12). The hydrology and topography of the watershed have made the areas most affected by flooding be the strategic infrastructure

"In-Guezzam airport" and its neighboring areas such as Abalag, BinaRifi, and Kounta. These areas remained flooded for 72 hours after the rain event (Fig. 5). The preferred water flow direction is oriented toward the airport and In-Guezzam City, which shows the heterogeneity of the spatial distribution that characterizes the flash flood.
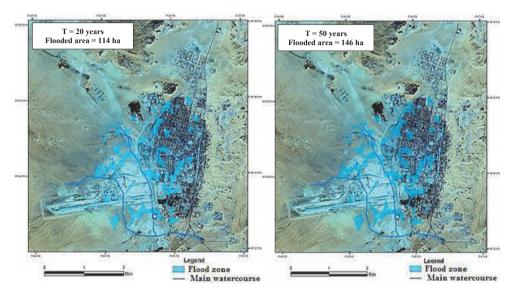

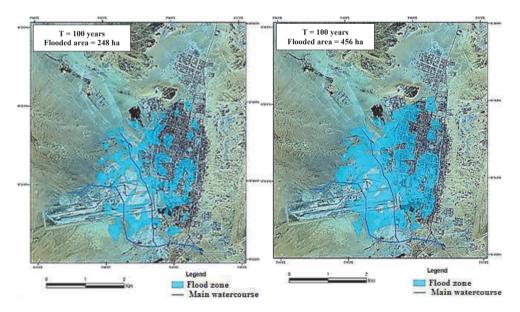**Fig. 11.** Flood vulnerability maps (20–50 years)

Fig. 12. Flood vulnerability maps (100–1000 years)

According to ASAL [66], laden water in some flooded areas at the decline on the city's northwest side indicates the mud and solid transport of materials accompanying the flood. Fifteen days after the flood, tiny water traces remained northwest of the city and at the airport. The disappearance of water traces in the urban area is complete [66].

6.7. Urbanization and Risk Analysis

Like all urban agglomerations, the In-Guezzam City had a spatial evolution of the urbanized area due to demographic and economic growth. The urban area has increased from 187 ha to 435 ha in eight years (2005–2013), then to 684 in 2019, i.e., almost three times in 15 years (Fig. 13). An urban extension is often carried out regardless of development plans and urban strategies. It was oriented towards the watercourse bed of Sahb El-Rahala.
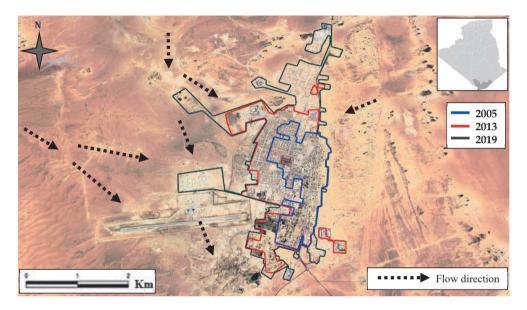

Fig. 13. Evolution of In-Guezzam urban expansion over time

Examining the flood hazard map of In-Guezzam City is developed by applying the HEC-RAS model, coupled with GIS using several parameters such as flooded areas, water depth, and soil type. Topography allows us to emerge. The spatial distribution of the degree of vulnerability to flooding in the city of In-Guezzam ranges from low to high. It is noted that areas of high vulnerability occupy 64.6% of the study area, which is located mainly at the strategic infrastructure "In-Guezzam airport", the agricultural area of Abalak, and the west of the city due to their location at the bottom of the Sahb El-Rahala watercourse. Although the medium vulnerability

indices are located north of the city center, their situation is below the slope, representing 22.2% of the city's surface.

This paper identifies three cities with low flood risks: Konta, EL-Khamsin, and Lebrark, which represent only 13% of the city surface. This situation requires moving urban expansions to the city's east side in the future to avoid material and human losses. This spatial approach to vulnerability enables emergency response to protect the city from flooding (Fig. 14). It provides support for decision-making in planning and land-use planning.
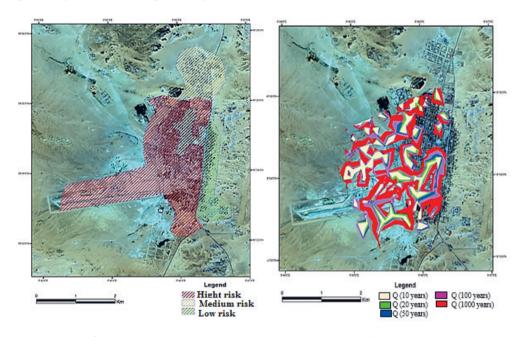

Fig. 14. Flood risk and vulnerability map in the city of In-Guezzam

7. Conclusion

In-Guezzam City is one of the Algerian-Nigerian border towns. It is located in a depressed area of Sahb El-Rahala and Adakh-Adakh watercourses. Its location strongly contributes to its vulnerability to flooding. Its watershed covers an area of 170 km² in the largest Sahara in the world. The In-Guezzam August 2018 flood was the most significant flood since 1997, with 53 mm; all city areas were affected by the flood. Over 272 ha, representing 41% of the total urban area, was affected on the first day. This flood has caused significant damage and loss of human and material resources.

The analysis of high-resolution Alsat-2 satellite images taken by the Algerian Space Agency after 72 hours of the rain event made it possible to provide more precise information concerning flooded areas at the scale of inhabited urban areas and major

infrastructure (airports, roads). It shows that the preferred water flow direction is oriented towards the airport and In-Guezzam City, with flooded areas of around 480 ha.

The first part of this work was devoted to the effect of climate change by studying the variability of annual and monthly scales rainfall series. This study has been done by applying the Mann–Kendall test and Sen's slope estimator at In-Guezzam meteorological station; the last one has detected a positive trend (Sen's slope = +1.175 mm/year) over the past three decades. On the other hand, the study of the mean annual temperatures is also carried out. The magnitude of warming has been significant over the last thirty years. It was also presented with a positive trend in the annual average (Sen's slope = +0.0512°C/year). This significant warming is mainly due to an increase in the summer average, which has been steadily increasing worldwide. These results can be used as a tool factor for controlling development work, preparing warning programs against the risks caused by floods whose damage is irreversible, and even quantifying eroded land.

The second part of this work was dedicated to the flood risk assessment, carried out via three analyses. The first is the frequency analysis of precipitation based on 30 years of maximum daily rainfall to develop the intensity-duration-frequency (IDF) curves for the different return periods 5, 10, 20, 50, 100, and 1,000 years. The hydrological analysis was carried out using EV3-Min (Weibull, L-Moments) distribution to calculate the flood recurrence. It was followed by applying the Giandotti method to transform the maximum daily rainfall of the different return periods into the flood flow, which is mainly related to the calculation of the concentration time, estimated to be at (5.0–5.5 h), and the runoff coefficient. The results show that the large catchment area has a significant centennial flow of around 162 m^3/s and a millennium that reached 391 m^3/s.

The hydraulic analysis is based on the input and output relationship through the HEC-RAS hydraulic model simulating the risk of flooding and mapping the ephemeral river. From flood maps, one can conclude that the flooded area develops with more extended return periods, ranging from around 114 ha in the case of a 20-year return period and flooding up to 456 ha in the case of a return period of 1,000 years, which represents 64.6% of the urban area.

This study is expected to provide a better understanding of the flooding process in the extreme south of Algeria, which could improve the use and effectiveness of risk assessment in disaster management and decision-making in the region. Nevertheless, one can note that some possible limitations could be addressed in future research. the main weakness lies in the lack of hourly data on flow rates and rainfall. This lack can considerably impact the calibration and validation of the model. More catchments should also be studied to further validate the model's suitability in other regions of the country, specifically in the arid regions. Further developments of this work will be addressed to real-time flood forecasting applications by considering the implementation of a soil moisture module to enable continuous modeling if continuous data are available.

Author Contributions

Rachid Zegait: research concept and design, data analysis and interpretation; writing the article; critical revision of the article; final approval of the article.

Zekai Şen, Antonio Pulido-Bosch: writing the article.

Housseyn Madi, Bachir Hamadeha: collection and assembly of data; data analysis and interpretation.

References

[1] Walls S.C., Barichivich W.J., Brown M.E.: *Drought, Deluge, and Declines: The Impact of Precipitation Extremes on Amphibians in a Changing Climate*. Biology, vol. 2(1), 2013, pp. 399–418. https://doi.org/10.3390/biology2010399.

[2] Madsen H., Lawrence D., Lang M., Martinkova M., Kjeldsene T.R.: *Review of trend analysis and climate change projections of extreme precipitation and floods in Europe*. Journal of Hydrology, vol. 519 (part D), 2014, pp. 3634–3650. https://doi.org/10.1016/j.jhydrol.2014.11.003.

[3] Kastridis A., Stathis D., Sapountzis M., Theodosiou G.: *Insect Outbreak and Long-Term Post-Fire Effects on Soil Erosion in Mediterranean Suburban Forest*. Land, vol. 11(6), 2022, 911. https://doi.org/10.3390/land11060911.

[4] Szewrański S., Chruściński J., Van Hoof J., Kazak J.K., Świąder M., Tokarczyk-Dorociak K., Żmuda R.: *A location intelligence system for the assessment of pluvial flooding risk and the identification of stormwater pollutant sources from roads in suburbanized areas*. Water, vol. 10(6), 2018, 746. https://doi.org/10.3390/w10060746.

[5] Ritter J., Berenguer M., Park S., Sempere-Torres D.: *Real-time assessment of flash flood impacts at pan-European scale: The ReAFFINE method*. Journal of Hydrology, vol. 603, 2021, 127022. https://doi.org/10.1016/j.jhydrol.2021.127022.

[6] Saharia M., Kirstetter P.E., Vergara H., Gourley J.J., Hong Y., Giroud M.: *Mapping flash flood severity in the United States*. Journal of Hydrometeorology, vol. 18(2), 2017, pp. 397–411. https://doi.org/10.1175/JHM-D-16-0082.1.

[7] Sapountzis M., Kastridis A., Kazamias A.-P., Karagiannidis A., Nikopoulos P., Lagouvardos K.: *Utilization and uncertainties of satellite precipitation data in flash flood hydrological analysis in ungauged watersheds*. Global NEST Journal, vol. 23(3), 2021, pp. 388–399. https://doi.org/10.30955/gnj.003905.

[8] Faccini F., Luino F., Paliaga G., Sacchini A., Turconi L., de Jong C.: *Role of rainfall intensity and urban sprawl in the 2014 flash flood in Genoa City, Bisagno catchment (Liguria, Italy)*. Applied Geography, vol. 98, 2018, pp. 224–241. https://doi.org/10.1016/j.apgeog.2018.07.022.

[9] Gaume E., Bain V., Bernardara P., Newinger O., Barbuc M., Bateman A., Blaškovičová L. et al.: *A compilation of data on European flash floods*. Journal of Hydrology, vol. 367(1–2), 2009, pp. 70–78. https://doi.org/10.1016/j.jhydrol.2008.12.028.

[10] Merz B., Kreibich H., Schwarze R., Thieken A.: *Review article "Assessment of economic flood damage"*. Natural Hazards and Earth System Sciences, vol. 10(8), 2010, pp. 1697–1724. https://doi.org/10.5194/nhess-10-1697-2010.

[11] Gaume É., Bain V., Borga M.: *Les crues éclair en Europe – Le projet de recherches Hydrate. Bulletin des laboratoires des ponts et chaussées (BLPC),* no. 277, 2010, pp. 65–73. https://www.ifsttar.fr/collections/BLPCpdfs/blpc_277_65-73.pdf [access: 13.02.2021].

[12] Lastrada E., Cobos G., Torrijo F.J.: *Analysis of Climate Change's Effect on Flood Risk. Case Study of Reinosa in the Ebro River Basin.* Water, vol. 12(4), 2020, 1114. https://doi.org/10.3390/w12041114.

[13] Diakakis M., Andreadakis E., Nikolopoulos E.I., Spyrou N.I., Gogou M.E., Deligiannakis G., Katsetsiadou N.K. et al.: *An integrated approach of ground and aerial observations in flash flood disaster investigations. The case of the 2017 Mandra flash flood in Greece.* International Journal of Disaster Risk Reduction, vol. 33, 2019, pp. 290–309. https://doi.org/10.1016/j.ijdrr.2018.10.015.

[14] IRIN (Integrated Regional Information Networks): *Preparing for floods in West Africa.* 2013. http://www.irinnews.org/report/98221/preparing-for-floods-in-west-africa [access: 13.02.2021].

[15] Moawad M.B., Abdel Aziz A.O., Mamtimin B.: *Flash floods in the Sahara: a case study for the 28 January 2013 flood in Qena, Egypt.* Geomatics, Natural Hazards and Risk, vol. 7(1), 2016, pp. 215–236. https://doi.org/10.1080/19475705.2014.885467.

[16] OCHA (United Nations Office for the Coordination of Humanitarian Affairs): *Sudan: Situation Report.* Last updated: 5 September 2022. https://reports.unocha.org/en/country/sudan [access: 13.02.2021].

[17] Huet P., Martin X., Prime J., Foine P., Lauraine C., Cannard P.: *Retour d'expériences des crues de septembre 2002 dans les départements du Gard, de l'Hérault, du Vaucluse, des bouches du Rhône, de l'Ardèche et de la Drôme.* Inspection générale de l'Environnement, Paris 2003.

[18] Lefrou C., Martin X., Labarthe J., Varret J., Mazière B., Tordjoman R., Feunteun R.: *Les crues des 11, 12 et 13 novembre 1999 dans les départements de l'Aude, l'Hérault, les Pyrénées orientales et du Tarn.* Inspection générale de l'Environnement, Paris 2000.

[19] Re M.: *Topics annual review: natural catastrophes 2002.* Munich Reinsurance Group, Geoscience Research, Munich 2002.

[20] Nouaceur Z., Laignel B., Turki I.: *Changements climatiques au Maghreb: vers des conditions plus humides et plus chaudes sur le littoral algérien?* Physio-Géo. Géographie physique et Environnement, vol. 7, 2013, pp. 307–323.

[21] Kastridis A., Kamperidou V., Stathis D.: *Dendroclimatological Analysis of Fir (A. borisii-regis) in Greece in the frame of Climate Change Investigation.* Forests, vol. 13(6), 2022, 879. https://doi.org/10.3390/f13060879.

[22] Laborde J.P.: *Carte pluviométrique de l'Algérie du Nord à l'échelle du 1/500000, notice explicative*. Projet PNUD/ALG/88/021, Agence Nationale des Ressources hydrauliques, Alger 1993.

[23] Meddi H., Meddi M.: *Variabilité spatiale et temporelle des précipitations du nord-ouest de l'Algérie*. Géographia Technica, no. 2, 2007, pp. 49–55.

[24] Mohammed T., Al-Amin A.: *Climate change and water resources in Algeria: vulnerability, impact and adaptation strategy*. Economic and Environmental Studies, vol. 18(1), 2018, pp. 411–429. https://doi.org/10.25167/ees.2018.45.23.

[25] Bessaklia H., Ghenim A.N., Megnounif A., Martin-Vide J.: *Spatial variability of concentration and aggressiveness of precipitation in North-East of Algeria*. Journal of Water and Land Development, vol. 36(1), 2018, pp. 3–15. https://doi.org/10.2478/jwld-2018-0001.

[26] Merabti A., Meddi M., Martins D.S., Pereira L.S.: *Comparing SPI and RDI applied at the local scale as influenced by climate*. Water Resources Management, vol. 32(3), 2018, pp. 1071–1085. https://doi.org/10.1007/s11269-017-1855-7.

[27] Troin J.-F.: *Le grand Maghreb (Algérie, Libye, Maroc, Mauritanie, Tunisie): Mondialisation et construction des territoires*. Armand Colin, Paris 2006.

[28] Remini B.: *Algeria: the climate is changing, the water is becoming scarce; what to do?* LARHYSS journal, no. 41, 2020, pp. 181–221. http://larhyss.net/ojs/index.php/larhyss/article/view/719.

[29] Bachar K.: *L'intégration des dimensions environnementales et sociales dans les pratiques urbaines en Algérie: enjeux et perspectives*. Université du Maine, 2015. https://tel.archives-ouvertes.fr/tel-01264701/document [access: 13.02.2021].

[30] Zegait R., BenSaha H., Addoun T.: *Water management and the agricultural development constraints in the Algerian Sahara: Case of the M'Zab Valley*. Journal of Water and Land Development, vol. 50 (VI–IX), 2021, pp. 173–179. https://doi.org/10.24425/jwld.2021.138172.

[31] Ballais J.-L.: *Les villes sahariennes et les risques naturels*. [in:] Côte M. (ed.), *La ville et le désert: Le Bas-Sahara algérien*, IREMAM – KARTHALA, 2005, pp. 59–71.

[32] Dubost D.: *Écologie, Aménagement et Développement Agricole des Oasis Algériennes*. Centre de Recherche Scientifique et Technique sur les Régions Arides, Biskra 2002 [Ph.D. thesis].

[33] ONM (*Office Nationale de la Météorologie*): *records listing of climatological parameters in the In-Guezzam region (1988–2019)*. Tamanrasset, Algeria 2019.

[34] Dubief J.: *Essai sur l'hydrologie superficielle au Sahara*. Université d'Alger, 1953 [Ph.D. thesis].

[35] Mann H.B.: *Nonparametric tests against trend*. Econometrica, vol. 13, 1945, pp. 245–259. https://doi.org/10.2307/1907187.

[36] Kendall M.G.: *Rank Correlation Methods*. Charles Griffin, London 1948.

[37] Sen P.K.: *Estimates of the regression coefficient based on Kendall's tau*. Journal of the American Statistical Association, vol. 63(324), 1968, pp. 1379–1389. https://doi.org/10.1080/01621459.1968.10480934.

[38] Faye C.: *Changement climatiques observés sur le littoral sénégalais (Région de Dakar) depuis 1960: Étude de la variabilité des tendances sur les températures et la pluviométrie*. Nature & Technology, C, Environmental Sciences, vol. 20, 2019, pp. 65–78.

[39] Patra J.P., Mishra A., Singh R., Raghuwanshi N.S.: *Detecting rainfall trends in twentieth century (1871–2006) over Ornoa State, India*. Climatic Change, vol. 111(3–4), 2012, pp. 801–817. https://doi.org/10.1007/s10584-011-0215-5.

[40] Sarailidis G., Vasiliades L., Loukas A.: *Analysis of streamflow droughts using fixed and variable thresholds. Hydrological Processes.* Hydrological Processes, vol. 33(3), 2019, pp. 414–431. https://doi.org/10.1002/hyp.13336.

[41] Shadmani M., Marofi S., Roknian M.: *Trend analysis in reference evapotranspiration using Mann–Kendall and Spearman's Rho tests in arid regions of Iran*. Water Resources Management, vol. 26(1), 2012, pp. 211–224. https://doi.org/10.1007/s11269-011-9913-z.

[42] Taxak A.K., Murumkar A.R., Arya D.S.: *Long term spatial and temporal rainfall trends and homogeneity analysis in Wainganga basin, Central India*. Weather and Climate Extremes, vol. 4, 2014, pp. 50–61. https://doi.org/10.1016/j.wace.2014.04.005.

[43] Fniguire F., Laftouhi N.-E., Saidi M.E., Zamrane Z., El Himer H., Khalil N.: *Spatial and temporal analysis of the drought vulnerability and risks over eight decades in a semi-arid region (Tensift basin: Morocco).* Theoretical and Applied Climatology, vol. 130, 2017, pp. 321–330. https://doi.org/10.1007/s00704-016-1873-z.

[44] Douglas E.M., Vogel R.M., Kroll C.N.: *Trends in foods and low flows in the United States: Impact of spatial correlation.* Journal of Hydrology, vol. 240(1–2), 2000, pp. 90–105. https://doi.org/10.1016/S0022-1694(00)00336-X.

[45] Da Silva R.M., Santos C.A., Moreira M., Corte-Real J., Silva V.C., Medeiros I.C.: *Rainfall and river flow trends using Mann–Kendall and Sen's slope estimator statistical tests in the Cobres River basin.* Natural Hazards, vol. 77(2), 2015, pp. 1205–1221. https://doi.org/10.1007/s11069-015-1644-7.

[46] Dawood M.: *Spatio-statistical analysis of temperature fluctuation using Mann–Kendall and Sen's slope approach.* Climate Dynamics, vol. 48(3), 2017, pp. 783–797. https://doi.org/10.1007/s00382-016-3110-y.

[47] Tabari H., Talaee P.H.: *Temporal variability of precipitation over Iran: 1966–2005.* Journal of Hydrology, vol. 396(3–4), 2011, pp. 313–320. https://doi.org/10.1016/j.jhydrol.2010.11.034.

[48] Vu T.M., Raghavan S.V., Liong S.Y., Mishra A.K.: *Uncertainties of gridded precipitation observations in characterizing spatio-temporal drought and wetness over Vietnam.* International Journal of Climatology, vol. 38(4), 2018, pp. 2067–2081. https://doi.org/10.1002/joc.5317.

[49] Salarijazi M., Akhon D., Ali A.M., Adib A., Daneshkhah A.: *Trend and change-point detection for the annual stream-flow series of the Karun River at the Ahvaz hydrometric station.* African Journal of Agricultural Research, vol. 7, 2012, pp. 4540–4552. https://doi.org/10.5897/AJAR12.650.

[50] Şen Z.: *Flood Modeling, Prediction, and Mitigation.* Springer, Cham 2018. https://doi.org/10.1007/978-3-319-52356-9.

[51] Viessman W.: *Introduction to Hydrology.* 5th ed. Prentice-Hall, Upper Saddle River, New Jersey 2003.

[52] Wang X., Melesse A.M.: *Evaluation of the SWAT model's snowmelt hydrology in a northwestern Minnesota watershed.* Transactions of the ASAE, vol. 48(4), 2005, pp. 1359–1376. https://doi.org/10.13031/2013.19194.

[53] Debo T.N., Reese A.J.: *Municipal Stormwater Management.* 2nd ed. Lewis Publishers, New York 2003.

[54] Nash J.E.: *River flow forecasting through conceptual models: A discussion of principles.* Journal of Hydrology, vol. 10(3), 1970, pp. 282–290. https://doi.org/10.1016/0022-1694(70)90255-6.

[55] Hapuarachchi H.A.P, Wang Q.J, Pagano T.C.: *A review of advances in flash flood forecasting.* Hydrological Processes, vol. 25(18), 2011, pp. 2771–2784. https://doi.org/10.1002/hyp.8040.

[56] Nalbantis I., Efstratiadis A., Rozos E., Kopsiafti M., Koutsoyiannis D.: *Holistic versus monomeric strategies for hydrological modeling of human-modified hydro systems.* Hydrology and Earth System Sciences, vol. 15(3), 2011, 743. https://doi.org/10.5194/hess-15-743-2011.

[57] Hydrognomon: *A Database System for the Management of Hydrometeorological Stations and Time Series. Hydrological Time Series Analysis and Processing Software Application.* 2012. https://hydrognomon.org [access: 14.08.2022].

[58] Cunnane C.: *Review of Statistical Models for Flood Frequency Estimation: Proceedings of the International Symposium on Flood Frequency and Risk Analyses, 14–17 May 1986, Louisiana State University, Baton Rouge, U.S.A.* [in:] Singh V.P. (ed.), *Hydrologic Frequency Modeling,* D. Reidel Publishing Company, Dordrecht 1987, pp. 49–95. https://doi.org/10.1007/978-94-009-3953-0_4.

[59] Body K.: *Analyse fréquentielle des pluies de l'Algérie: Synthèse régionale: détermination des paramètres principaux par station et leur répartition spatiale.* Institut National des Ressources hydrauliques INRH, Constantine 1985.

[60] SEDAT *(*Société des etudes diverses & assistance technique): *Etude du schéma directeur d'assainissement de la ville d'In-Guezzam, Mission II.* Etude Topographique, 2013.

[61] Brunner G.W.: *HEC-RAS River Analysis System Hydraulic Reference Manual (Version 3.1 Edition).* U.S. Army Corps of Engineers Hydrologic Engineering Center, Davis, California 2002.

[62] McKay G.A.: *Precipitation.* [in:] Gray D.M. (ed.), *Handbook on the Principles of Hydrology: With Special Emphasis Directed to Canadian Conditions in the Discussions, Applications and Presentation of Data,* Secretariat, Canadian National Committee for the International Hydrological Decade, Ottawa 1970, pp. 12–111.

[63] Tarek D., Azzedine H., Mouldi S.: *Predetermination of Floods by Different Methods. Case of the El Kébir-West Watershed in Ain-Charchar (Northeast Algeria).* Synthèse: Revue des Sciences et de la Technologie, vol. 34, 2017, pp. 74–84.

[64] ABHS (Agence de bassin hydrographique Sahara): *Etude du cadastre hydraulique de bassin hydrographique du Sahara, Rapport Mission 1: ressources en eau et en sol*. 2006.

[65] Lahsaini M., Tabyaoui H.: *Modelisation Hydraulique Mono Dimensionnel Par HEC RAS, Application Sur L'oued Aggay (Ville De Sefrou).* European Scientific Journal, vol. 14, no. 18, 2018, pp. 110–121. https://doi.org/10.19044/esj.2018.v14n18p110.

[66] ASAL (Agence Spatiale Algérienne): *Impacts des inondations dans la région d'In Guezzam – Wilaya de Tamanrasset, à partir de l'imagerie satellitaire à moyenne résolution Alsat-1B et haute résolution Alsat-2*. 2018.